JOURNAL OF MASS SPECTROMETRY, VOL. 32, 689–696 (1997)

Conformation of Doubly Protonated Peptides Studied by Charge-separation Reactions in Mass Spectrometry

Zoltán Szilágyi, László Drahos and Károly Vékey*
Central Research Institute for Chemistry, Hungarian Academy of Sciences, Pusztaszeri út 59–67, H-1025 Budapest, Hungary

Charge-separation metastable processes were investigated by mass spectrometry and kinetic energy release (KER) distributions were determined from the measured metastable peak profiles. Benzene, *p*-*N*,*N*-dimethylaminoaniline and pipecuronium bromide (Arduan) were investigated as reference compounds to confirm that there is a well defined relationship between the KER distribution and the distance of the two charged centers. For these 'rigid' systems relatively narrow KER distributions were found, and the average values were in good agreement with the intercharge distances determined by a semi-empirical (MNDO) molecular orbital calculation. Two metastable processes of bradykinin, a nonapeptide and one of trilysine were studied. The distribution of KER suggests that the conformation of bradykinin is fairly rigid, whereas that of trilysine is flexible. The observed KER values clearly indicate far smaller intercharge distances than those corresponding to extended geometries. This is clear experimental evidence that medium-sized doubly charged peptides have a folded and not an extended geometry in the gas phase. © **1997 by John Wiley & Sons, Ltd.**

J. Mass Spectrom. **32**, 689–696 (1997)
No. of Figures: 5 No. of Tables: 1 No. of Refs: 48

KEYWORDS: tandem mass spectrometry; kinetic energy release; peptides; conformation; molecular orbital calculations (MNDO)

INTRODUCTION

In the last decade, mass spectrometry has become an indispensable tool in peptide and protein research. In addition to the molecular mass, tandem mass spectrometry relatively easily yields information on the amino acid residues, and often the whole sequence can be determined.[1–3] Multiply protonated peptides are often studied (Refs 4–8 and references cited therein), commonly generated by electrospray ionization.[9,10] The conformation of peptides is less easy to study by mass spectrometry, although there are several interesting approaches: charge-state distribution in electrospray;[10–15] collision cross-sections (ion chromatography or ion mobility);[11,16,17] reactivity, e.g. by H–D exchange;[10,18–25] direct determination of molecular shape from ion-impact features;[26] and theoretical calculations.[27–29] These suggest that the conformation of proteins or large peptides in the gas phase relates to that in solution, and can be studied by mass spectrometry.

The conformation of small- and medium-sized peptides in the gas phase is even less well understood. That of doubly protonated peptides is of particular interest in gas-phase ion chemistry. Their conformation is significantly influenced by Coulomb repulsion, U.[4,27,30–32] Depending on the distance of protonation sites, Coulomb repulsion is typically in the range 40–200 kJ mol^{-1}, which is a very significant amount of energy. This leads to the suggestion that, to minimize Coulomb repulsion, multiply protonated peptides assume an extended (β-sheet, extended or 'linear') conformation.[27] This assumption is widely accepted, even though experimental studies[28,33–36] and theoretical modeling[16,17,28,29] suggest the contrary.

Probably the first suggestion that doubly charged peptides may have folded geometries came from an early study on doubly protonated bradykinin.[33] The kinetic energy release (KER) observed in the fragmentation suggested an intercharge distance of $\sim$1.5 nm, much smaller than the length of the molecule in an extended conformation ($>$3.6 nm). Further experimental support came from studies on doubly protonated adducts fragmenting into protonated monomers.[34–36] The corresponding KER is large, indicating much smaller intercharge distances, than those corresponding to fragmentation of compounds in an extended conformation. A recent study determining KER distributions also indicates that intercharge distances are smaller than the length of the peptide in an extended conformation.[28] This work showed that protonation does not necessarily occur on the two terminal residues but also on other residues in a doubly protonated peptide.

Theoretical modeling of peptide conformations is plagued by the fact that the accuracy of calculation and

* *Correspondence to*: K. Vékey, Central Research Institute for Chemistry, Hungarian Academy of Sciences, Pusztaszeri út 59–67, H-1025 Budapest, Hungary.

CCC 1076–5174/97/070689–08 $17.50

Received 2 January 1997
Accepted 14 March 1997

the size of the compound which can be studied are inversely related. The highest accuracy obtained at present on a doubly protonated peptide is a recent *ab initio* molecular orbital study on tetraglycine, using full geometry optimization.[29] For larger peptides, full geometry optimization is possibly only at the semi-empirical level. Molecular mechanic and dynamic calculations have the advantage of exploring a large part of the conformational hyperspace, but the accuracy of relative energetics (e.g. comparison of extended and folded geometries) is not reliable. Often parts of the molecule are optimized using a molecular orbital method, then these parts are joined together and used as inputs for molecular dynamic calculations.[16,17,28] All of these studies suggest that folded conformations are more likely in the case of doubly protonated peptides than the extended conformer. The *ab initio* study on doubly protonated tetraglycine strongly suggests that the folded geometry is energetically more stable, in spite of the larger Coulomb repulsion, than the extended (β-sheet) conformation. These studies point out the importance of intramolecular solvation, especially that of the protonated site, on the stability of doubly protonated compounds.

In the present paper, the conformation of doubly protonated peptides is addressed based on experimental evidence on the KER observed in fragmentation processes. The results are evaluated using techniques established in gas-phase ion chemistry for small molecules. Using pipecuronium bromide (Arduan), a bisquaternary steroid, it is shown that these techniques can also be used to derive accurate information of the gas-phase structure of large molecules. To understand the techniques used, possible sources of error and uncertainties in the case of large molecules, the KER and its determination, the Coulomb energy in a doubly charged ion and the connection between these values are discussed in some detail below.

The Coulomb energy (U) among charges is expressed, in the general case, by the following equation:[30–32,37–39]

$$U = \sum_i \sum_j U_{ij} = \sum_i \sum_j c \frac{q_i q_j}{r_{ij}} \quad (1)$$

where i and j are the charged sites, U_{ij} is the Coulomb energy between charges q_i and q_j, r_{ij} is the distance between the two charges and c is a conversion constant (equal to 1.439 if charges are given in units of electron charge, r in nm and energy in eV). The Coulomb energy between two parts of an ion can be calculated by the same equation, provided that i represents charges in one part and j in the other part of the ion. Charges in ions are typically 'delocalized,' and in such a case the ion is characterized by a charge density (fractional charges centered at various nuclei). This presents no fundamental problem in the application of Eqn (1); the sums should go through the individual fractional charges in the ion.

In the case of protonation, the charge density is often closely centered on the protonated 'heavy' atom (e.g. nitrogen), so assuming a point charge at the formal position of the charge is usually a good approximation.[40] If there are only two, localized, charges in the ion, Eqn (1) simplifies to

$$U = \frac{c}{r_{ij}} \quad (2)$$

r_{ij} being the distance between the two (unit) charges.

If a dielectric is present between the two charges, the Coulomb repulsion will be reduced by the dielectric constant of the medium ($\varepsilon \geqslant 1$). It is a macroscopic effect, and the dielectric constant within a molecule strictly has no meaning (i.e. $\varepsilon = 1$, relating to vacuum, should be used). The total energy of a system calculated by the Schrödinger equation does not use a dielectric constant calculating the Coulomb energy, so there is no reason to use it in Eqn (1) or (2), which are certain fractions of the total energy. The recent suggestion of using an 'intrinsic dielectric constant' for rationalizing the results of proton transfer experiments[30–32] may serve to compensate for neglecting ion–induced dipole interactions or the large energy barrier to proton transfer in multiply charged species.[4]

The KER of a charge separation process has a distribution, but most often a single KER value characterizing this distribution is used. The value most often determined is that corresponding to the half-height of the metastable peak ($T_{0.5}$). The main advantage of using $T_{0.5}$ is that its determination is easy and reproducible. In the case of dish-topped peaks (typical for a charge separation process), $T_{0.5}$ was shown to be close to the average KER ($\langle T \rangle$ or T_{ave}) and to the most probable KER value (T_{mp}).[39] Sometimes the KER is measured at the horns of a metastable peak, but that strongly depends on the resolution (especially on the length of the z slit) and is usually not a good approximation of $\langle T \rangle$ or T_{mp}. In principle, the use of $\langle T \rangle$ or T_{mp} is more desirable than $T_{0.5}$, but their determination is fairly complicated. The KER distribution (KERD) has to be determined first, and $\langle T \rangle$ and T_{mp} can then be determined from this distribution.

The KERD is determined from the metastable peak shape by computer programs, several of which have been described.[41–44] The metastable peak shape has to be known with a good signal-to-noise (S/N) ratio for the determination of KERD (much higher than that for $T_{0.5}$), requiring high sensitivity. Instrument resolution and discrimination should also to be taken into account. Excessive smoothing of the metastable peak may distort (widen) the peak shape, so this should be avoided. Errors related to extensive smoothing may be even larger than differences among $T_{0.5}$, T_{mp} and $\langle T \rangle$, which are often within 10–20% in the case of dish-topped peaks. The main advantages of determining KERD instead of using $T_{0.5}$ are that the information derived is more reliable, depends less on instrument parameters (e.g. resolution) and may give information on the conformational flexibility of the system.

The KER (usually $T_{0.5}$) observed in charge-separation reactions of small doubly charged ions have long been used to determine the distance of charges in the transition state.[4,37–39,45] In the evaluation it is usually assumed that the KER originates solely from Coulomb repulsion and that all of the Coulomb energy appears as KER. These were confirmed in a recent study combining theoretical calculations with experimental data on small aromatics.[39]

EXPERIMENTAL

Mass spectrometric measurements were performed on a reverse-geometry VG ZAB2-SEQ instrument. Metastable peak profiles were observed using mass-analyzed ion kinetic energy (MIKE) spectra. In this work, six metastable processes of five compounds were investigated: benzene and *p-N,N*-dimethylaminoaniline by electron impact (EI) ionization and Arduan, trilysine and bradykinin by fast atom bombardment (FAB) ionization. All the compounds are commercially available.

In the mass spectrometric experiments, an accelerating voltage of 4030 V and a resolution of 2000 were used. In EI measurements the ionizing electron energy was 70 eV. In FAB measurements, a cesium atom gun was used at 30 kV energy, the samples were dissolved in glycerol matrix and the intensity of doubly charged ions was increased by the addition of hydrochloric acid.[46]

The observed metastable peak profiles were analyzed by our computer program developed for the determination of KERD.[44] The algorithm used in the program is based on the calculation of the velocity of the ions formed in the metastable process. The program calculates the 'ideal' trajectory of the product ion in the instrument with some assumptions (infinitely narrow source slit, a monoenergetic parent ion beam with no angular dispersion, etc.). Peak broadening due to instrumental effects is taken into account by the program using the experimentally observed peak shape of the main beam. Discrimination effects, which are typically significant for KER values larger than 0.2–0.3 eV, are also taken into account by the algorithm. Discrimination, causing 'dishing' of the metastable peaks, is due to the fact that product ions with large angular divergence hit the walls of the instrument and so are not detected. The program was thoroughly tested and the results were compared with data published in the literature. The treatment of discrimination, particularly important for charge separation processes, and peak broadening due to instrumental effects was checked with particular care, using both experimental and simulated data. The program uses no initial estimate for the KERD, runs automatically (does not need parameters which have to be determined by a trial and error procedure) and requires few input parameters: the instrument geometry, angular transmittance of the electrostatic analyser, the accelerating voltage, mass of the parent ion, metastable and main beam peak profiles.

Semi-empirical computations were performed using the standard MNDO method of Dewar and Thiel.[47] Calculations were performed using the MOPAC (version 6.0) software package (Frank J. Seiler Research Laboratory, US Air Force Academy, Colorado Springs, CO, USA). Starting geometries were obtained by MM^+ molecular mechanics calculations using the HyperChem Molecular Modeling System (version 3.0) (Hypercube).

RESULTS AND DISCUSSION

First, the shape of the KER distribution of charge separation processes occurring in molecules with a rigid skeleton was checked. For this purpose, three compounds were chosen: benzene, *p-N,N*-dimethylaminoaniline and Arduan (Fig. 1). Benzene is a well studied example, the KER values corresponding to the process

$$[\text{benzene}]^{2+} \rightarrow [C_5H_3]^+ + [CH_3]^+ \quad (3)$$

were reported to be in the range 2.6–3.0 eV, determined by various techniques.[41–43] The KER distribution was reported recently[44] (using the same experimental set-up and data evaluation as in the present work), and is reproduced in Fig. 2(a). From this $\langle T \rangle = 2.91$ eV and $T_{mp} = 2.87$ eV can be determined, which can be compared with $T_{0.5} = 2.77$ measured from the peak profile directly (Table 1). The reported KER values are close to the reverse critical energy (2.43 eV) and to the Coulomb energy in the transition state (2.70 eV) calculated by the MNDO method.[39] The T values reported correspond to an intercharge distance between 0.49 and 0.52 nm.

The KERD was calculated[44] in the case of another small aromatic molecule, *p-N,N*-dimethylaminoaniline, for the process

$$[p\text{-}N,N\text{-dimethylaminoaniline}]^{2+} \rightarrow [C_6H_7N]^+ + [C_2H_5N]^+ \quad (4)$$

The shape and width of the KER distribution are fairly similar to those of benzene, and are shown in Fig. 2(b). $T_{mp} = 2.91$ eV, the related parameters are given in Table 1 and the intercharge distance calculated from T_{mp} using Eqn (2) is 0.49 nm.

The third and most important, compound used as a standard in determining intercharge distances is Arduan (Fig. 1). It is a relatively large, rigid molecule. The two charges are expected to be well 'localized' at the two quaternary nitrogens. This is confirmed by an MNDO calculation showing that ~90% of the charge is in the first coordination sphere around the quaternary nitrogen (the nitrogen plus the four neighboring carbons, including the attached hydrogens). Placing unit charges at the quaternary nitrogens, the intercharge distance will be equal to the distance between the two nitrogen atoms (1.61 nm, determined by x-ray studies[48]). Full geometry optimization using the MNDO technique results in a very similar distance (1.66 nm) between the two quaternary nitrogens. The doubly charged molecular ion of Arduan fragments by the following unimolecular charge separation process:

$$[\text{Arduan-2Br}]^{2+} \rightarrow [C_{31}H_{52}N_3O_4]^+ + [C_4H_{10}N]^+ \quad (5)$$

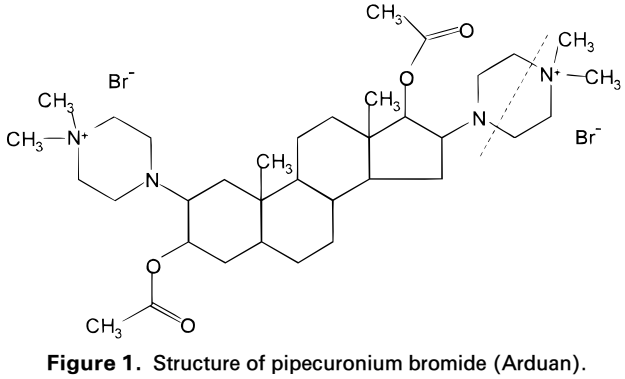

Figure 1. Structure of pipecuronium bromide (Arduan).

Table 1. KER data ($T_{0.5}$, and T_{mp}) and intercharge distances determined for the metastable processes studied

Compound	Metastable process[a]	$T_{0.5}$ (eV)	KER $\langle T \rangle$ (eV)	T_{mp} (eV)	Intercharge distance from T_{mp} (nm)
Benzene	$78^{2+} \rightarrow \underline{63}^{+} + 15^{+}$	2.77	2.91	2.87	0.50
p-*N*,*N*-Dimethylaminoaniline	$136^{2+} \rightarrow \underline{93}^{+} + 43^{+}$	2.92	2.97	2.91	0.49
Arduan	$602^{2+} \rightarrow \underline{530}^{+} + 72^{+}$	1.05	1.04	0.94	1.53
Bradykinin (process 6)	$1061^{2+} \rightarrow \underline{1002}^{+} + 59^{+}$	0.98	0.99	0.88	1.64
Bradykinin (process 7)	$1061^{2+} \rightarrow \underline{974}^{+} + 87^{+}$	1.03	1.02	0.95	1.51
Trilysine	$404^{2+} \rightarrow \underline{275}^{+} + 129^{+}$	1.30	1.15	1.12	1.28

[a] The studied metastable peak is underlined.

The KERD corresponding to this process is shown in Fig. 2(c); T_{mp} is 0.94 eV (Table 1). The intercharge distance calculated from T_{mp} is 1.53 nm, agreeing within 10% with the distance between the two nitrogens in the equilibrium geometry. We believe that this is the first experimental demonstration that the KER gives a good numerical estimate of the intercharge distance in large molecules. This is also an experimental indication that it is unnecessary to assume a dielectric (and consequently an 'intrinsic' dielectric constant) within an ion for calculation of the Coulomb energy.

The $\langle T \rangle$ value of the charge separation reactions is always larger than T_{mp}, but $\langle T \rangle$, T_{mp} and $T_{0.5}$ for the reactions discussed above are fairly close, within 10% of each other (Table 1). The reproducibility of $\langle T \rangle$ and T_{mp} values is $\sim$5%, that of $T_{0.5}$ is somewhat better, but the latter value depends on the instrument and on the resolution. The reproducibility depends mainly on the S/N ratio of the metastable peak, and also on the presence of interfering signals (e.g. overlapping peaks). The KERD curves (Fig. 2) have very similar shapes and widths (the full width at half-height being $\sim$0.7 eV). The reason why a distribution, and not a single KER value, is observed is due to several effects: (i) the reverse critical energy and the Coulomb energy in the transition state are similar, but not precisely equal,[39] and each influences the KER; (ii) a small and variable fraction of the Coulomb energy in the transition state may be converted into internal energy (and not to KER); (iii) part of the excess energy in the transition state will be converted into KER; (iv) ion–dipole and ion–induced dipole interactions may affect the amount of Coulomb energy converted into KER; (v) various conformers of the parent ion are likely to react through slightly different reaction channels, presumably resulting in slightly different KER, causing a broadening of the KER distribution (in other words, even the 'rigid' molecules studied here are not completely rigid). Effects (i)–(v) result in the distribution of KER observed in Fig. 2.

The results discussed here and in previous papers (Ref. 39 and references cited therein) support the contention that the correlation between KER, the Coulomb energy and intercharge distance holds reasonably well. The correlations are, however, not so straightforward as to allow precise and reliable determination of the intercharge distance. It is difficult to decide *a priori* which part of the KER distribution should be used to determine the intercharge distance. Results on the test compounds suggest that a value close to T_{mp} may be the best approximation, but $\langle T \rangle$ and $T_{0.5}$ values could also be used. The authors believe that (with our present understanding) intercharge distances can be determined only with an accuracy of $\sim \pm 20\%$ based on KER or KERD. The reproducibility can, however, be much better (in the present work $\sim \pm 5\%$, mainly depending on the S/N ratio), so changes in the intercharge distances can be monitored with better precision. The previously detailed results suggest that T_{mp} values are in good agreement with the equilibrium geometry determined by semi-empirical methods and/or by x-ray crystallography. This is true in spite of the fact that KER reflects transition-state properties. It seems likely that $\langle T \rangle$ would correlate fairly well with the transition-state

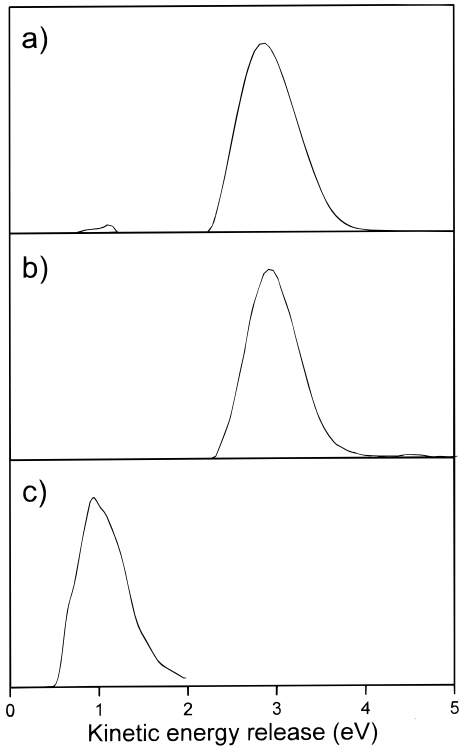

Figure 2 Kinetic energy release distributions calculated from the metastable peak profiles of the reference (rigid) systems: (a) benzene; (b) *p*-*N*,*N*-dimethylaminoaniline; (c) pipecuronium bromide (Arduan).

geometry, but the determination of the latter is not straightforward.

Following these test cases, two unimolecular charge separation reactions of doubly charged bradykinin, a nonapeptide (RPPGFSPFR) having arginine residues at the C and N termini, were studied. The two by far the most basic residues are the two arginine residues. Coulomb repulsion also favors protonation at the furthest residues, so double protonation is certain to occur on the two arginine side-chains. The doubly protonated molecule has two reaction channels producing abundant products by charge separation:

$$[\text{bradykinin} + 2\text{H}]^{2+} \rightarrow [\text{C}_{49}\text{H}_{70}\text{N}_{12}\text{O}_{11}] + [\text{CH}_5\text{N}_3]^+ \quad (6)$$

$$[\text{bradykinin} + 2\text{H}]^{2+} \rightarrow [\text{C}_{47}\text{H}_{66}\text{N}_{12}\text{O}_{11} + [\text{C}_3\text{H}_9\text{N}_3]^+ \quad (7)$$

Both fragmentation channels correspond to cleavage at the side-chain of an arginine residue, giving further support for the protonation site. The two metastable peaks corresponding to the high-mass fragments are shown in Fig. 3(a) and the corresponding KER distributions in Fig. 3(b) and the T values are listed in Table 1. The two processes give slightly but reproducibly different T_{mp} values; the corresponding intercharge distances are 1.64 and 1.51 nm, respectively.

The distance between the two protonated sites (the —NH—C^+—$(NH_2)_2$ units) in the fully extended geometry is >3.6 nm (calculated by molecular mechanics). The intercharge distance determined from KERD is less than half of this value, as discussed above. This unequivocally indicates that doubly protonated bradykinin, in spite of the Coulomb repulsion, assumes a folded geometry in the gas phase, emphasizing the importance of intramolecular solvation.

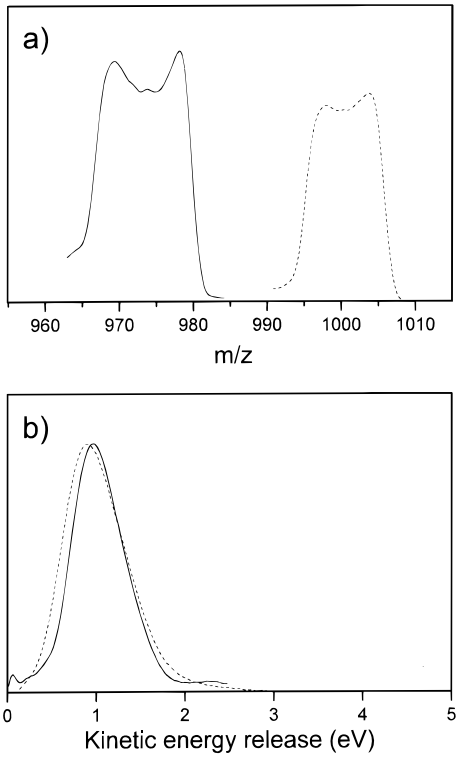

Figure 3. (a) Metastable peak profiles of the two investigated metastable decompositions of doubly protonated bradykinin (solid curve, process 7; dashed curve, process 6). (b) Calculated kinetic energy release distributions (solid curve, process 7; dashed curve, process 6).

The geometry of doubly protonated bradykinin was also calculated by a semi-empirical (MNDO) calculation. Starting from an extended (β-sheet) structure, full geometry optimization retains the extended conformation. The structure is shown in Fig. 4(a); the distance of the formally charged carbons atoms is 3.53 nm. Figure 4(a) shows that even in this extended geometry the protonated arginine side-chain [at the left-hand side of Fig. 4(a)] folds back to form H-bridges. Full MNDO geometry optimization starting from an α-helix type starting configuration results in the folded structure shown in Fig. 4(b), which is characterized by a much shorter intercharge distance (1.57 nm). Probably there are hundreds of other possible conformers, some probably of lower energy. This result indicates that the folded structure shown in Fig. 4(b) may occur in the gas phase and does not spontaneously open to an extended geometry, which is in good agreement with the KER measurements. It is emphasized that in these calculations all internal coordinates are optimized at the MNDO level, i.e. these are (relative to the large size of the ion) high-accuracy calculations, much better than those typically used in molecular dynamics.

The shape and the width of the KERD curve for process (7) is similar to those of the rigid test compounds, and for process (6) it is only slightly wider. This suggests that the conformation of doubly protonated bradykinin is nearly as rigid as that of the reference compounds. This can be explained with the strong intramolecular solvation effects discussed above, which fix the intercharge distance to a fairly well defined value.

Trilysine is a small peptide having four alternative protonation sites of similar basicity (the N terminus and the three lysine side-chains). The doubly protonated molecule fragments by the following charge separation process, resulting in an intense metastable peak:

$$[\text{trilysine} + 2\text{H}]^{2+} \rightarrow [\text{C}_{12}\text{H}_{27}\text{N}_4\text{O}_3]^+[\text{C}_6\text{H}_{13}\text{N}_2\text{O}]^+ \quad (8)$$

In this process, the amide bond between the first and the second amino acid residues is cleaved. The KERD calculated for this process is shown in Fig. 5(a) (solid curve). T_{mp} is 1.12 eV and the corresponding intercharge distance is 1.28 nm. This is much smaller than the length of the molecule in a fully extended geometry, where Coulomb repulsion is minimized. (The distance of the furthest nitrogen atoms in the extended geometry is 1.98 nm, calculated by molecular mechanics.)

The KER distribution in the case of trilysine is significantly wider than in the case of the reference compounds or bradykinin discussed above. This suggests that reaction (8) proceeds through several alternative channels, characterized by different intercharge distances. The most likely explanation for this is that the doubly protonated molecule in this case has a very flexible conformation, and/or there is a distribution of isomers protonated at various positions. It is reasonable

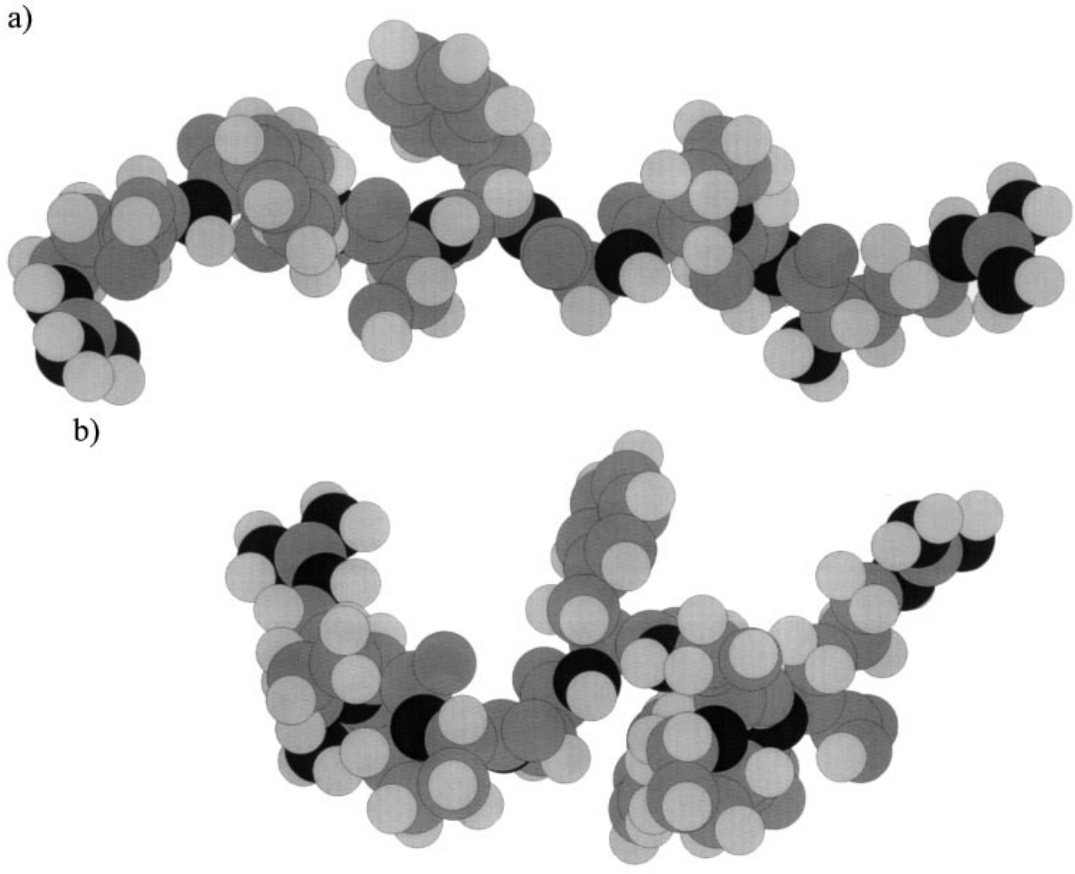

Figure 4. MNDO-optimized structures of bradykinin doubly protonated at the two arginine residues. (a) Extended (β-sheet) and (b) folded (α-helix) conformations.

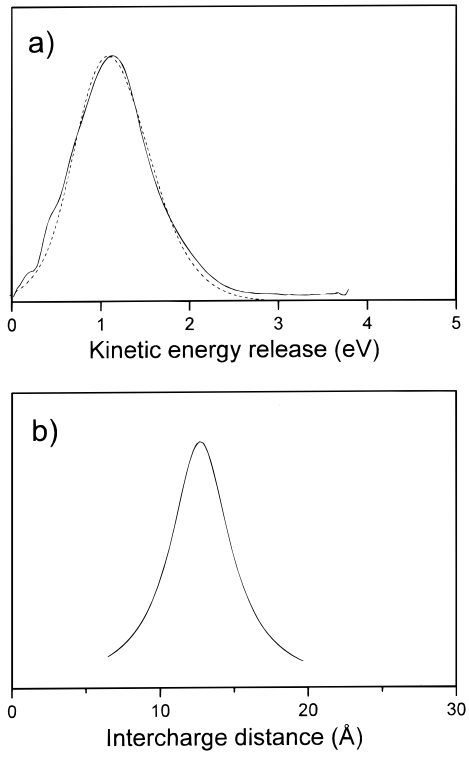

Figure 5. (a) Kinetic energy release distribution of doubly protonated trilysine corresponding to process 8 (solid curve). The KERD curve recalculated by convolution of Figs 5(b) and 2(a) is also shown (dotted curve). (b) Intercharge distance distribution of doubly protonated trilysine calculated from the kinetic energy release distribution.

to assume that a rigid system results in a KER distribution similar to that of the compounds discussed above, as suggested by the shapes and widths of the KERD curves shown in Figs 2 and 3. Using this assumption, the KERD curve observed for trilysine should be due to the convolution of the intercharge distance distribution with the KERD curve corresponding to a rigid molecule.

The intercharge distance distribution of trilysine can, therefore, be determined by deconvolution of the observed KERD curve [Fig. 5(a), solid curve] and that corresponding to a rigid molecule [e.g. that of benzene, Fig. 2(a)]. Using manual deconvolution (a trial and error procedure), the distribution of intercharge distances was determined in the case of trilysine, and is shown in Fig. 5(b). The accuracy of deconvolution can be estimated by recalculating the KERD curve of trilysine from the intercharge distance distribution [Fig. 5(b)] and KERD curve of benzene [Fig. 2(a)]. This is done by convolution using a simple computer program, and the result is shown in Fig. 5(a) (dashed curve). The experimentally obtained and the recalculated KERD curves show good agreement.

Trilysine was also modeled by MNDO calculations. It is assumed in the following that the charges are centered at the protonated nitrogens. Charge distributions in trilysine obtained by MNDO calculations indicated that this is a good approximation. Starting from an extended geometry, protonated at the side-chains of the two terminal residues, full geometry optimization results

in a 1.75 nm intercharge distance. If the side-chains of two neighbouring residues are protonated, the (MNDO-optimized) intercharge distance is 1.51 nm. If the amide nitrogens at the cleavage site and on the furthest other nitrogen (side-chain of the *N*-terminal lysine) are protonated, MNDO optimization results in a small (1.12 nm) intercharge distance (in this case the charge is shifted to the carbonyl during fragmentation).

The calculated geometries can be compared with the intercharge distance distribution obtained from KERD. The shape of the distribution [one maximum, smooth curve, Fig. 5(b)] cannot be explained by a mixture of two or three well defined 'rigid' structures (or transition states). It rather suggests a very flexible, fairly folded conformation and the presence of a mixture of several isomeric structures (double protonation at various combinations of possible locations).

CONCLUSIONS

Charge separation processes, common in doubly and multiply charged compounds, are accompanied by a large KER. These give information on the intercharge distance in the transition state. In those cases when the protonation site is known, the intercharge distance characterizes the conformation of the molecule. In this work we evaluated the metastable peak shape to determine the KER distribution,[44] from this the most probable KER value (T_{mp}), and from this, using Eqn (2), the intercharge distance. This procedure is preferred to that using the metastable peak width directly ($T_{0.5}$), as the latter depends more on the instrument geometry and on experimental parameters, and seems less reliable. The experimental approach used here is similar to that described recently,[28] although it uses a different program[44] to determine KERD.

The novelty in the present work is the use of a large, rigid reference compound (Arduan), with well defined charge locations. This shows that T_{mp} defines the distance between the two charged sites in the ion to within $\pm 10\%$. To be on the safe side, we estimate that the distance between protonated sites can be determined with better than $\pm 20\%$ accuracy using the present approach. The reproducibility is much better ($\sim \pm 5\%$). We believe that this is the first experimental demonstration that T_{mp} gives a numerically correct estimate for the distance of the charged (protonated) sites in large compounds using Eqn (2).

The other novelty is the use of a model peptide, bradykinin, where the two protonation sites are unambiguous. The basicity differences among amino acid residues, distances between protonation sites and the fragmentation processes observed all indicate protonation at the side-chain of the two terminal arginine residues. In such a case, the observed intercharge distance (calculated from Eqn (2) using T_{mp}) characterizes the conformation (degree of folding) of the doubly protonated molecule in the gas phase. The results clearly show that doubly protonated bradykinin has a rigid, folded conformation, characterized by a 1.5–1.6 nm intercharge distance. This is far smaller than the intercharge distance in the extended conformation (3.53 nm). These results point to the importance of internal solvation effects in gas-phase ions.

The results for trilysine show that not only T_{mp} but also the width of the KER distribution contains important information on molecular conformation. While the rigid reference compounds and bradykinin have very similar KERD peak widths, that of trilysine is much wider. This is interpreted as a sign of the conformational flexibility of the doubly charged ion in the gas phase. From the KERD peak shape an intercharge distance distribution can be extracted [Fig. 5(b)].

Acknowledgements

The authors are grateful to the Hungarian Research Fund for providing support (OTKA No. F016774 and C0020).

REFERENCES

1. K. F. Medzihradszky and A. L. Burlingame, *Compan. Methods Enzymol* **6**, 284 (1994).
2. I. A. Papayannopoulos, *Mass Spectrom. Rev.* **14**, 49 (1995).
3. K. Biemann and S. A. Martin, *Mass Spectrom. Rev.* **6**, 1 (1987).
4. K. Vékey, *Mass Spectrom. Rev.* **14**, 195 (1995).
5. D. Fabris, M. Kelly, C. Murphy, Z. Wu and C. Fenselau, *J. Am. Soc. Mass Spectrom.* **4**, 652 (1993).
6. X. Tang and R. K. Boyd, *Rapid Commun. Mass Spectrom.* **6**, 651 (1992).
7. X.-J. Tang, P. Thibault and R. K. Boyd, *Anal. Chem.* **65**, 2824 (1993).
8. D. F. Hunt, N. Zhu and J. Shabanowitz, *Rapid Commun. Mass Spectrom.* **3**, 122 (1989).
9. J. B. Fenn, M. Mann, C. K. Meng, S. F. Wong and C. M. Whitehouse, *Science* **246**, 64 (1989).
10. R. D. Smith, J. A. Loo, R. R. O. Loo, M. Busman and H. R. Udseth, *Mass Spectrom. Rev.* **10**, 359 (1991).
11. K. A. Cox, R. K. Julian, Jr, R. G. Cooks and R. E. Kaiser, Jr, *J. Am. Soc. Mass Spectrom.* **5**, 127 (1994).
12. J. A. Loo, R. R. O. Loo, H. R. Udseth, C. G. Edmonds and R. D. Smith, *Rapid Commun. Mass Spectrom.* **5**, 101 (1991).
13. U. A. Mirza, S. L. Cohen and B. T. Chait, *Anal. Chem.* **65**, 1 (1993).
14. S. K. Chowdhury, V. Katta and B. T. Chait, *J. Am. Chem. Soc.* **112**, 9012 (1990).
15. J. A. Loo, R. R. O. Loo and P. C. Andrews, *Org. Mass Spectrom.* **28**, 1640 (1993).
16. G. Helden, T. Wyttenbach and M. T. Bowers, *Science* **267**, 1483 (1995).
17. G. Helden, T. Wyttenbach and M. T. Bowers, *Int. J. Mass Spectrom. Ion Phys.* **146/147**, 349 (1995).
18. B. E. Winger, K. J. Wahl-Light, A. L. Rockwood and R. D. Smith, *J. Am. Chem. Soc.* **114**, 5897 (1992).
19. V. Katta and B. T. Chait, *Rapid Commun. Mass. Spectrom.* **5**, 214 (1991).
20. C. Brown, P. Camilleri, N. J. Haskins and M. J. Saunders, *J. Chem. Soc., Chem. Commun.* 761 (1992).
21. D. Suckau, Y. Shi, S. C. Beu, M. W. Senko, J. P. Quinn, F. M. Wampler and F. W. McLafferty, *Proc. Natl. Acad. Sci. USA* **90**, 790 (1993).
22. O. R. R. Loo, J. A. Loo, H. R. Udseth, J. L. Fulton and R. D. Smith, *Rapid Commun. Mass Spectrom.* **6**, 159 (1992).

23. O. R. R. Loo and R. D. Smith, *J. Am. Soc. Mass Spectrom.* **5**, 207 (1994).
24. D. Suckau, M. Mák and M. Przybylski, *Proc. Natl. Acad. Sci. USA* **89**, 5630 (1992).
25. C. Borchers, D. Suckau, M. Mák and M. Przybylski, *Fresenius' J. Anal. Chem.* **343**, 64 (1992).
26. C. T. Reimann, A. P. Quist, J. Kopniczky, B. U. R. Sundqvist, R. Erlandsson and P. Tengvall, *Nucl. Instrum. Methods Phys. Res., Sect. B* **88**, 29 (1994).
27. A. L. Rockwood, M. Busman and R. D. Smith, *Int. J. Mass Spectrom. Ion Processes* **111**, 103 (1991).
28. J. Adams, F. H. Strobel, A. Reiter and M. C. Sullards, *J. Am. Soc. Mass Spectrom.* **7**, 30 (1996).
29. K. Vékey and A. Gömöry, *Rapid. Commun. Mass. Spectrom.* **10**, 1485 (1996).
30. D. S. Gross and E. R. Williams, *J. Am. Chem. Soc.* **117**, 883 (1995).
31. P. D. Schnier, D. S. Gross and E. R. Williams, *J. Am. Chem. Soc.* **117**, 6747 (1995).
32. D. S. Gross, S. E. Rodriguez-Cruz, S. Bock and E. R. Williams, *J. Phys. Chem.* **99**, 4034 (1995).
33. K. Vékey, M. Candido and P. Traldi, *Rapid Commun. Mass Spectrom.* **4**, 74 (1994).
34. I. A. Kaltashov, D. Fabris and C. C. Fenselau, *J. Phys. Chem.* **99**, 10046 (1995).
35. I. A. Kaltashov and C. C. Fenselau, *J. Am. Chem. Soc.* **117**, 9906 (1995).
36. I. A. Kaltashov and C. C. Fenselau, *Rapid Commun. Mass Spectrom.* **10**, 857 (1996).
37. R. G. Cooks, J. H. Beynon, R. M. Caprioli and G. R. Lester, *Metastable Ions*. Elsevier, Amsterdam (1973).
38. T. Ast, *Adv. Mass Spectrom.* **8**, 555 (1980).
39. K. Vékey and G. Pócsfalvi, *Org. Mass Spectrom.* **27**, 1203 (1992).
40. L. Drahos and K. Vékey, in preparation.
41. B. A. Rumpf and P. J. Derrick, *Int. J. Mass Spectrom. Ion Phys.* **82**, 239 (1988).
42. G. K. Koyanagi, J. Wang and R. E. March, *Rapid Commun. Mass Spectrom.* **4**, 373 (1990).
43. Y. J. Lee, H. Y. So and M. S. Kim, *Rapid Commun. Mass Spectrom.* **8**, 571 (1994).
44. Z. Szilágyi and K. Vékey, *Eur. Mass Spectrom.* **1**, 507 (1995).
45. J. H. Beynon and A. E. Fontaine, *Chem. Commun.* 717 (1966).
46. M. Barber, D. J. Bell, M. Morris, L. W. Tetler, M. D. Woods, J. J. Monaghan and W. E. Morden, *Org. Mass Spectrom.* **24**, 504 (1989).
47. M. J. S. Dewar and W. Thiel, *J. Am. Chem. Soc.* **99**, 4899 (1977).
48. Z. Tuba, S. Mahó, L. Párkányi and M. Czugler, presented at the International Symposium on Steric Aspects of Biomolecular Interactions, 26–29 August 1985, Sopron, Hungary (Abstract P II-9).

